Pile group behavior under unsymmetrical cyclic thermal loading in dry silty sand: 1g Physical modeling

Fardin Jafarzadeh[1], Sina Afzalsoltani[2]*

Abstract

The effect of unsymmetrical thermal loading on the behavior of 2×2 pile groups is studied using 1g physical modeling. Three tests were conducted with 1, 2 and 3 energy piles in each pile group to apply the cyclic unsymmetrical thermal load. Model piles were closed-end aluminum pipes and the model ground was fine-grained dry silty sand, placed in the container with dry tamping technique. 10 successive heating-cooling cycles with amplitude of ±6°C were applied to the energy piles. Displacements and rotations of the cap, axial forces and bending moments along the piles, changes in soil pressure under the pile tip and temperature distribution around the group are monitored and discussed in detail. A new parameter, named as "pile tip behavior index" (I_{pt}) is introduced to determine the elastic/plastic state of the soil under the pile tip during each test. Results suggest that build-up of plastic zones in the soil under the energy pile during first stages of the unsymmetrical thermal cycling along with redistribution of the mechanical surcharge among different piles of each group may contribute to cause unallowable rotations of the pile cap.

Keywords: Energy piles, Thermo-Mechanical behavior, Pile groups, Unsymmetrical thermal loading, Physical modeling

1. Introduction

Traditional piles have been studied using physical modeling technique in several studies [1-5]. The behavior of energy piles as a form of energy geo-structures has gained increasing scholarly attention in recent years. Some researchers directed their effort to assess the thermal efficiency of energy piles and to reveal the involved parameters [6-10]. Some researchers investigated the behavior of energy piles using field scale tests [11-15] or model scale tests [16-23]. Sutman et al. [24] also studied the effect of end and head restraint condition on the behavior of energy piles using a field test and reported that the thermo-mechanical behavior of energy piles, that is to say, axial displacements, mobilized shaft resistance and thermal stresses are highly associated with the restraint conditions on both ends of the pile. Ng et al. [25] studied the effect of temperature increase on a floating aluminum pile in saturated sand using centrifuge tests. They observed a pile head heave of 0.4%D and 1%D and an increase of 13% and 30% in pile overall capacity as a result of 15°C and 30°C increase in pile temperature; respectively. Nguyen et al. [26] studied the long-term behavior of single

[1] Fardin Jafarzadeh, Chairman of Iranian Geotechnical Society (IGS) and Associate Professor, Department of Civil Engineering, Sharif University of Technology, Tehran, Iran. Fardin@Sharif.ir

[2] Sina Afzalsoltani, Ph. D. Candidate, Department of Civil Engineering, Sharif University of Technology, Tehran, Iran. S.Afzalsoltani@gmail.com- Corresponding Author

aluminum energy piles in dry sand through 1g physical modeling. They reported that thermal cycling under constant mechanical load induces irreversible pile head settlement with the largest settlement increment occurring in the first thermal cycle. They also stated that thermal cycling did not induce noticeable changes in total pressures in soil underneath the pile base. Ng et al. [17] conducted a centrifuge modeling of pile spacing effects on thermo-mechanical interactions between piles within energy pile groups. They concluded that a pile spacing of 5D is preferable over a spacing of 3D in terms of serviceability limits satisfaction. Ng et al. [18] compared the behavior of non-symmetrical thermally loaded 2×2 elevated pile group with a piled raft. They stipulated that piled rafts undergo smaller tilts under unsymmetrical thermal loads. Senejani et al. [16] investigated thermo-mechanical behavior of a single energy pile using a small-scale physical model setup. They reported a reduction in elastic response of the soil during longer thermal cycles. Foglia et al. [27] conducted large-scale model tests of a single pile and two-pile groups for an offshore platform in sand. The study found that the pile spacing and pile group configuration significantly affect the bearing capacity and settlement of the energy pile group. Yang et al. [28] conducted physical model tests and numerical simulations to evaluate the effects of different factors on the thermo-mechanical behavior of an energy pile group. The study found that the pile spacing, pile diameter, and soil thermal conductivity significantly affect the thermal response of the energy pile group.

The above-mentioned studies, highlight the importance of conducting physical or full-scale model tests to evaluate the thermo-mechanical behavior of energy pile groups. Generally, physical model tests are time consuming; hence, most of the experimental studies on energy piles had only included short term behavior of piles with less than four thermal cycles. Therefore, the present study aims to contribute into this domain by applying 10 successive heating-cooling cycles to account for long-term behavior of energy pile groups. Moreover, the readings from the total pressure cells below each pile tip were adopted to introduce a new parameter which is used to describe the elastic/plastic state of the soil under the pile tip. Pile displacements, rotations of the cap and stresses along each pile are monitored and discussed in detail.

2. Physical Model

2.1. Model configuration and test plan

The model contains a 2×2 pile group (each pile with outer diameter of D=2 cm) placed at a center-to-center distance of 6cm (3D). The soil container is a 100×100×80 cm (width × length × height) rigid steel box. The model ground is dry silty sand with relative density of 74%, placed in the container using dry tamping technique. Figure 1 shows the schematic of the model configuration and Figure 2 depicts the constructed model.

Pile temperature is controlled by circulating temperature-controlled water through steel U-tubes placed inside the piles. In order to provide sufficient thermal interaction between pile and U-tube, each pile is initially filled with water. The pile group was first mechanically loaded in 8 steps up to 400 N with resting time of 5 minutes for each step (the loading shaft itself weights 1.5 kg). Under constant mechanical surcharge, the energy pile has gone through 10 consecutive heating-cooling cycles with temperature amplitude of

±6˚C. Three tests were conducted. In test "Group1", Pile1 was energy pile and the other piles were non-energy piles. In test "Group2", Pile1 and Pile2 were energy piles and finally in test "Group3", Pile1, Pile2 and Pile3 were energy piles. After each test the whole model was reconstructed. Test plan is outlined in Table 1.

Particle size distribution of the model ground is depicted in Figure 3. As can be seen the model ground is comprised of fine sand and 40% passing from #200 sieve. Results of Atterberg tests showed the part finer than #200 sieve is non-plastic silt. Hence the soil based on the Unified Soil Classification System is SM.

2.2. Model scaling and material selection

Studying the scaled-down model of an intended prototype, needs the scaling factors for different involved parameters to be defined. Iai [29] introduced a similitude law for 1g shake table tests. Even though the present study is kinematic in its nature, the scaling factors from Iai [29] are applicable to this study as well regarding the adopted 1g modeling space. In order to include thermal parameters in the similitude law, we have assumed that the material used in the model has the same specific heat capacity as that of prototype. In a centrifuge test, this assumption automatically results in a scaling factor of 1 for temperature changes; however, in 1g field, considering the scaling factor of 1 for temperate alongside with the former assumption forces the thermal energy to have a different scaling factor than mechanical energy. Obviously, it is neither possible nor necessary to exactly scale down every single parameter in a model test; hence, since the energy efficacy aspect of energy piles is of less importance in the present study, a scaling factor of 1 is assumed for temperature. It is also assumed that the strains throughout the test remain in a small range (less than 10^{-6}) which leads to a scaling factor of $\lambda_\varepsilon = \lambda^{0.5}$ for the strains, with λ being the geometric scaling factor. This assumption might be erroneous if strains become large enough, for example in case of pile failure. Iai et al. [30] suggested that when the stress-strain behavior of soil is available through laboratory tests for the entire range of strains, the scaling factor for the strain can be directly obtained from the results of those tests.

Considering the limitations in model dimensions and test materials, a geometric scale factor of 20 is adopted in the present study. Heat-exchanger pipes can be fitted inside either driven piles or cast-in-place concrete ones. Typically, it is more convenient to construct cast-in-place concrete piles especially in urban areas as their construction, as opposed to driven ones, neither needs special machinery nor makes considerable vibration and noise pollution. Prototype energy piles in the present study is assumed to be cylindrical cast-in-place concrete piles with 12 m in length and a diameter of 60 cm. Given the geometric scale factor of 20 and other scaling factors as outlined in Table 2, the required model pile specifications can now be derived mathematically. Considering the theoretically calculated properties for the model piles and the materials available at the market, Aluminum pipes of 60 cm length and 2 cm diameter are chosen as model piles. Table 3 briefly outlines the mechanical specifications of the prototype and model piles. It is noteworthy that due to higher thermal expansion coefficient of Aluminum in comparison to concrete, the results from this study might be exaggerated and care should be taken in extrapolation of the results to the prototype.

3. RESULTS

3.1. Pile behavior under sole mechanical loading

Figure 4 shows time history of head displacements for different piles of the group during mechanical loading at room temperature (21.5°C) in test "Group1". As can be seen, even though equal load increments were applied to the pile group in each loading step, yet larger settlements were observed during early steps of the mechanical loading. This can be attributed to the activation of sleeve friction along the piles and possible increase in soil elastic modulus under the pile tip due to compaction.

Profiles of axial load for selected piles of the group in each test, as shown in Figure 5, indicate activation of the sleeve friction as stepwise mechanical loading continues (note that the slope of the profiles decrease with an increase in the mechanical head load in each test until it becomes constant after a pile head load of 65N). The axial load profile corresponding to the smallest head load (from loading plate and its shaft) has a convex shape denoting negative (downward) sleeve friction along the upper half of the pile length which is generated during compaction of the soil in the vicinity of the pile during model construction. It is also noteworthy that the gentler slope of the profile in the deeper parts is due to higher normal stresses applied to the pile perimeter which in return generate larger traction forces on the pile.

Comparison of parts a, b and c of Figure 5 with each other indicates that the same construction method was successfully executed for each test as the same load distribution pattern was observed along the "Pile1" of each test (other piles also showed the same results yet are not presented for brevity.).

3.2. Temperature distribution

During the tests, the room temperature variation was limited to ±0.5°C. The energy piles were connected to the temperature-controlled water circulation system, allowing their temperature to oscillate with amplitude of ±6°C between successive heating and cooling cycles. The water-filled non-energy piles however, where not connected to any temperature control device and the variations in their temperature is caused by the temperature changes of the energy piles.

Temperature variation of the surrounding soil is recorded by 12 thermocouples installed at different elevations and radial distances from the piles (refer to Figure 1 for the location of sensors T1 to T12). temperature contours are calculated based on the data obtained from the uppermost layer of thermocouples (T1 to T5 in Figure 1) and are shown in Figure 6. These contours are obtained by interpolating the readings of the thermocouples, using Gaussian process regression (also known as Wiener-Kolmogorov prediction or Kriging method [31]). It can be seen that in all tests, non-energy piles acted as thermal barriers. This is due to the fact that all piles (even the non-energy piles) are initially filled with water which has a larger specific heat capacity relative to the surrounding soil; hence it would take more energy to change the pile temperature relative to the surrounding soil.

3.3. Pile cap displacements

Four linear displacement transducers are installed on the pile cap at four corners to monitor displacements of the piles and rotations of the cap (Figure 2). As shown in Figure 2, in order to avoid interference of displacement sensors with the loading plate, the sensors are not connected to the cap exactly above the location of the corresponding piles; however, in order to obtain head displacements of each pile in the group, reading of each displacement sensor is transformed to the location of the corresponding pile head. In order to do so, first, the equation of the cap's plane in space is obtained using the readings of displacement sensors at each time and then the elevation of the top of each pile (z) is calculated by inserting the x-y coordinates of that pile in the equation of the cap's plane.

Time histories of total pile head displacements during each test are presented in Figure 7. It can be seen that in each test, the energy piles have larger settlements than conventional piles of the group; the larger the number of the energy piles in the group is, the larger settlements are observed. In tests "Group2" and "Group3", heating caused a heave in energy piles while cooling caused settlement. The magnitude of incremental displacements in each heating/cooling phase becomes smaller with an asymptotic trend as the cycling goes on. In test "Group1", during the first few heating phases, no upward displacement occurs in the energy pile until the third heating phase in day five of the test. In fact, during first and second heating phases, the upward thermal forces generated by the tendency of the energy pile for expansion, cannot overcome the downward reaction forces from the conventional piles of the group. As thermal cycling continues, settlement of the energy pile and the consequent redistribution of forces acting on the pile contribute to help the energy pile to slightly push the pile cap upwards which is recorded as small heaves during heating phases in Figure 7-a. It can be seen from Figure 7 that the magnitude of total settlement of each pile (regardless of the tilt in the cap) in tests "Group1", "Group2" and "Group3" remains smaller than the maximum allowable settlement, which is conventionally taken as 10% of the pile diameter (2mm).

Figure 8 shows time histories of the cap rotation and its tilt for tests "Group1", "Group2" and "Group3". The tilt can be calculated by dividing the relative vertical displacements of any two points on the cap, by the horizontal distance between them in the tilting direction. As can be seen, almost in all cases, heating caused a decrease while cooling caused an increase in the tilt of the cap. The exceptions are twofold: first, in all tests, the first heating phase induced a tilt in the cap with that being almost equal for tests "Group1" and "Group2" and being slightly larger for test "Group3". The second exception can be seen in test "Group1", where the second heating phase as well as the first heating phase caused a slight increase in the tilt of the cap. The amplitude of oscillations in the tilt of the cap is the largest for test "Group2" and the smallest for test "Group1". This amplitude becomes smaller with an asymptotic trend in tests "Group1" and "Group2" as the cycling continues but it seems to remain constant for test "Group3". As indicated in Figure 8, tilt of the cap in tests "Group1" and "Group2" exceeds allowable limit of 1/500 (0.2%) suggested by EN 1997-1

[32] in second and first cooling phases; respectively. In test "Group3" however, tilts of the cap touch the limit line in fourth cooling phase for the first time and marginally exceeds the allowable limit in the following cooling phases.

3.4. Axial force along piles

Axial force along the piles is recorded by full-bridge circuits of strain gauges installed at four elevations on each pile as shown on Figure 1. Temperature-induced axial forces or thermal axial forces along the piles at any time can be calculated by subtracting the initial forces just before the onset of thermal cycling from the measured axial forces at that specific time. Profiles of thermal axial forces for energy piles can be used to determine and track the location of null point during thermal cycling. According to Figure 9-a, the null point of the energy pile in test "Group1" is approximately at depth of 300 mm from the pile head (note that the sign of the profile slope changes at this depth). From the second heating cycle onwards, the location of null point has moved downwards to the depth of 400 mm in heating phases which implies that the lower half of the pile is taking more load share relative to the upper half. Location of the null point of energy piles in tests "Group2" and "Group3" remains almost at depth of 400 mm during all heating phases (Figure 10-a and Figure 11- a, b; respectively). Note that in all tests, the location of null point of energy piles almost remains constant at depth of 300 mm during cooling phases. From Figure 9 to Figure 11, it can be observed that the thermal axial force in non-energy piles does not change significantly with depth; meaning that thermal loading of energy piles does not noticeably affect the skin frictional forces on non-energy piles. However, profiles of thermal axial force for energy piles show that during heating phases, thermal axial force notably changes with depth denoting the effect of heating on friction forces acting on the pile sleeve. During cooling phases, thermal axial forces does not change significantly with depth along the energy piles except for diagonal energy piles in test "Group3" (Figure 11-b). Note that both of heating and cooling phases induce positive (compressional) thermal forces along the diagonal energy piles in test "Group3", except for the first two cooling phases which induce slight tensional forces in upper half of these piles.

Figure 12 shows distribution of group's total mechanical head load between the piles of each group (parts a, b and c of the figure) and also the share of each pile's tip from its head load (parts d, e and f of the figure). The share of each pile from the head load of the group is calculated by linearly extrapolating the axial forces measured by strain gauges to the top of each pile. The axial force at the pile tip was estimated in a similar manner. From Figure 12 (parts a to c), it can be observed that heating phases in general have increased the load share of the energy piles while cooling phases had reductive effect which can be attributed to thermal expansion/contraction of pile material. It was also found that the first stages of thermal cycling did not noticeably affect the load share of the energy pile/piles; however, after a few cycles the share of energy pile starts to increase more noticeably with each heating phase. As thermal cycling continues, irreversible increase in the load share of energy piles is accumulated. As mentioned earlier this can be attributed to compaction of the soil under the pile tip due to excessive settlement of the energy pile and the consequent increase

in soil elastic modulus in that region. At the beginning of all tests, Pile1 took 25% of the total mechanical load of pile group (as all other piles at the beginning of the test); at the end, this reached to 29.3%, 31.62% and 28.4% in tests "Group1", "Group2" and "Group3"; respectively. The share of diagonal energy piles (Pile2 and Pile3) in test "Group3" from total mechanical head load of the group reached to 31.4% at the end of the test for each pile.

In Figure 12 (parts d, e and f), it can be observed that for the energy piles, the share of pile tip from the estimated head load of the same pile, increases with each heating-cooling cycle. It can also be seen that in the majority of cases, heating of the energy pile caused an increase in the share of pile tip from its head load while cooling had a reductive effect. This can be attributed to thermal softening of the soil-pile interface during heating phases which happened at both the pile tip and the pile sleeve; however in the majority of cases, thermal softening at pile sleeve interface seems to dominate the softening at the pile tip interface (note that the opposite has happened in the first heating phase in tests "Group1" and "Group2" causing the share of the energy pile tip from its estimated head load to be reduced in Figure 12-d and e; respectively.). At the beginning of all tests, approximately 45% of each pile's head load reached to its tip. For Pile1 it increased to 64%, 60% and 56% by the end of tests "Group1", "Group2" and "Group3"; respectively. For the diagonal energy piles (Pile2 and Pile3) in test "Group3", it increased to 58% at the end of the test. These numbers do not seem to depend merely on the amount of settlement in the corresponding pile (refer to Figure 7) and possibly more complicated interactions are contributing to this behavior which demand farther studies to be fully understood.

3.5. Total soil pressure under the pile tip

Time histories of vertical soil pressure at depth of 4cm below the pile tip for different piles at each test are recorded by four total pressure cells (for sensor locations refer to Figure 1) and are plotted in Figure 13. It was observed that in all tests, with each heating/cooling phase the soil pressure under the energy pile has increased/decreased; respectively. The amplitude of soil pressure oscillations has increased gradually during the first few cycles until it remained almost constant after the fifth cycle. Moreover, in Figure 13, the back-calculated vertical soil pressure at the location of total soil pressure sensors were also plotted after estimation based on the Boussinesq [33] equation as follows:

$$\sigma_b^{Z_0} = q \times \left[1 - \frac{1}{\left[1 + \left(R / Z_0 \right)^2 \right]^{3/2}} \right] + \sigma_{ini}^{Z_0} \qquad \text{Eq. 1}$$

Where:

$\sigma_b^{Z_0}$ is the estimated vertical soil pressure at depth of Z_0 below the pile tip based on Boussinesq [33]- kPa

q is the uniform distributed load on a circular foundation (here, the pressure at the pile tip)- kPa

R is the radius of the pile tip- cm

Z_0 is depth of total pressure cell (TPC) measured from the pile tip- cm

$\sigma_{ini}^{Z_0}$ is the initial vertical soil pressure recorded by the total pressure cell- kPa

In the above equation, Boussinesq [33] assumed that the soil is a linear-elastic, homogenous, isotropic, semi-infinite medium. In the present study, an attempt was made to relate any deviation of the total cell pressure readings from the pressures estimated by Boussinesq [33] equation to deviation of the soil state from the assumptions made by Boussinesq [33]. Sadek and Shahrour [34] reported that the Boussinesq [33] equation underestimates stresses if the soil is in plastic state. According to Figure 13-a, the measured vertical stresses by the TPC under Pile4 in test "Group1" is almost the same as those estimated by Eq. 1, implying that the soil in that zone remained in elastic state during thermal cycling. Note that in test "Group1", the TPC readings under the energy pile during heating phases are larger than values estimated by Eq. 1 denoting that the soil is deviating from elastic state while during cooling phases TPC readings are relatively close to those estimated by Eq. 1.

4. FURTHER DISCUSSIONS

In order to gain a deeper insight into the behavior of the pile and especially the behavior of the soil under the pile tip, a parameter named as "pile tip behavior index" (I_{pt}) is introduced which is calculated as follows:

$$I_{pt} = \frac{\sigma_b^{Z_0} - \sigma_a^{Z_0}}{\sigma_b^{Z_0}} \times 100 \qquad \textit{Eq. 2}$$

In which:

I_{pt} is the pile tip behavior index (%);

$\sigma_b^{Z_0}$ is the estimated vertical soil pressure at depth of Z_0 below the pile tip based on Boussinesq [33]- kPa

$\sigma_a^{Z_0}$ is the soil pressure at a depth of Z_0 under the pile tip measured by a soil pressure sensor.

In other words, I_{pt} somehow may indicate deviance of the soil from elastic behavior; meaning that the larger the pile tip behavior index is, probably the more plastic the soil under the pile tip has become (note that one important assumption in Boussinesq [33] equations is that the soil remains an elastic homogenous medium.).

Time history of the pile tip behavior index for different piles during stepwise mechanical loading of the pile group is presented in Figure 14. Even though mechanical loading of the pile group was conducted with extreme caution to avoid sudden impacts on the cap, the spikes in this figure are corresponding to inevitable slight vibrations of the pile group in the process of adding surcharge weights.

As can be seen, the first 2-3 steps of loading caused an increase in the I_{pt} while farther loading of the pile group reduced this parameter which can imply an increase in soil elastic modulus due to compaction under the pile tip at larger head loads.

Time history of pile tip behavior index (I_{pt}) during thermal cycling for different piles of each test is plotted in Figure 15. The large spikes are corresponding to shocks caused by the thermal phase shift from heating to cooling or vice versa. Note that in tests "Group1" and "Group2", the I_{pt} for the energy piles has risen up to approximately 20% and has reduced again with the start of the first cooling phase. From the second thermal cycle onwards, the I_{pt} of the energy pile in test "Group1" remained close to zero which can be a sign of soil compaction under the pile tip after the first thermal cycle. In test "Group2" the I_{pt} of the non-energy piles has increased with each heating phase (especially after the third thermal cycle) and has decreased during cooling phases; in this test during the first three thermal cycles probably the soil under the energy piles was excessively compacting with each plastic settlement and consequently less energy was reached to the soil under the pile tip of non-energy piles which could be the reason of less increases of the I_{pt} for the non-energy piles during the early thermal cycles. Note that the I_{pt} of the non-energy pile in test "Group3" followed a similar pattern. In test "Group3", the changes of the I_{pt} for the energy piles are smaller relative to those observed for the energy piles of the other two tests. This can be attributed to less head restraint in test "Group3" due to fewer non-energy piles in the group.

5. Competing Interests

The Authors certify that they have no afflictions with of involvement in any organization or entity with any financial interest or non-financial interest in the subject matter or materials discussed in this manuscript.

6. Data Availability Statement

The datasets generated and/or analyzed during the current study are available from the corresponding author on reasonable request.

7. Conclusion

In the present study three 1g physical model tests on 2×2 pile groups were conducted to study the effect of unsymmetrical thermal loading on the behavior of the pile group. The pile groups are initially loaded in a stepwise manner to 400 N (415N considering the weight of the loading shaft) at constant temperature of 21.5°C. In tests "Group1", "Group2" and "Group3", one, two and three energy piles were used; respectively to apply an unsymmetrical thermal load to the group. Axial forces and bending moment along the piles of the group are recorded by full-bridge circuits of strain gauges. Displacements of the pile cap were recorded by four displacement sensors at each corner of the cap. Temperature distribution around the energy piles is monitored using several thermocouples at different locations around the pile group. Total soil pressure cells were used under each pile and their readings were

adopted to introduce a new parameter named as "pile tip behavior index" - I_{pt}. The introduced parameter is used to describe the elastic/plastic state of the soil under the pile tip. The summary of the most important findings of this study are as follows:

1- During the initial mechanical loading of the group, larger settlements were observed during first steps of the mechanical loading which can be attributed to the activation of sleeve friction along the piles and possible increase in soil elastic modulus under the pile tip due to compaction.

2- The magnitude of total settlement of each pile (regardless of the tilt in the cap) in all tests remains smaller than the maximum allowable settlement, which is conventionally taken as 10% of the pile diameter (2mm).

3- Tilt of the cap in tests "Group1" and "Group2" exceeds allowable limit of 1/500 (0.2%) suggested by EN 1997-1 [32] in second and first cooling phases; respectively. In test "Group3" however, the diagram corresponding to tilts of the cap touches the limit line in fourth cooling phase for the first time and marginally exceeds the allowable limit in the following cooling phases.

4- The null point of the energy pile in test "Group1" is initially located at an approximate depth of 300 mm from the pile head. From the second heating cycle onwards, the location of null point has moved downwards to the depth of 400 mm in heating phases which implies that the lower half of the pile is taking larger load share relative to the upper half. Location of the null point of energy piles in tests "Group2" and "Group3" remains almost at depth of 400 mm during all heating phases.

5- During cooling phases in all tests, the location of the null point of energy piles almost remains constant at depth of 300 mm below pile tip.

6- In energy piles, the majority of the heating phases caused an increase in the mobilized friction in upper parts of the pile (depths of 100 mm to 400 mm below the pile head) while having mostly a reductive effect on the mobilized sleeve friction at depths below 400 mm from the pile head.

7- The thermally induced bending moments and axial forces in the piles of this study are well below the yield limits of the pile material. However, due to cyclic nature of the thermal loading, fatigue effects which can build up cracks within the pile material over the long run, should be taken into account, regardless.

8- The introduced "pile tip behavior index"- I_{pt} was found to be useful in interpretation of the soil behavior under the pile tip.

9- During the initial mechanical loading of the group, the first 2-3 steps of loading caused an increase in the I_{pt} while farther loading of the pile group reduced this parameter which can imply an increase in soil elastic modulus due to compaction under the pile tip at larger head loads.

10- From the second thermal cycle onwards, the I_{pt} of the energy pile in test "Group1" remained close to zero which can be a sign of soil compaction under the pile tip after the first thermal cycle.

11- In tests "Group2" and "Group3" the I_{pt} of the non-energy piles has increased with each heating phase (especially after the third thermal cycle) and has decreased during cooling phases.

12- In test "Group3", the changes of the I_{pt} for the energy piles are smaller relative to those observed for the energy piles of the other two tests. This can be attributed to less head restraint in test "Group3" due to fewer non-energy piles in the group.

References

1. Haeri, S., Rajabigol, M., Salaripour, S., et al., *Effects of liquefaction-induced lateral spreading on a 3× 3 pile group using 1g shake table and laminar shear box*, in *Earthquake Geotechnical Engineering for Protection and Development of Environment and Constructions*. 2019, CRC Press. p. 2764-2770 DOI: https://doi.org/10.1201/9780429031274.
2. Haeri, S.M., Kavand, A., Raisianzadeh, J., et al., *Effectiveness of a vertical micro-pile system for mitigating lateral spreading damage on pile groups: 1g shake table tests*, in *Earthquake Geotechnical Engineering for Protection and Development of Environment and Constructions*. 2019, CRC Press. p. 3989-3996 DOI: https://doi.org/10.1201/9780429031274.
3. Haeri, S.M., Rajabigol, M., Salaripour, S., et al., *Effects of physical modeling boundary conditions on the responses of 3× 3 pile groups to liquefaction induced lateral spreading.* Bulletin of Earthquake Engineering, 2023. **21**(5): p. 2469-2502 DOI: https://doi.org/10.1007/s10518-023-01648-4.
4. Kavand, A., Haeri, S.M., Raisianzadeh, J., et al., *Effectiveness of a vertical micropile system in mitigating the liquefaction-induced lateral spreading effects on pile foundations: 1 g large-scale shake table tests.* Scientia Iranica, 2022. **29**(3): p. 1038-1058 DOI: https://doi.org/10.24200/sci.2021.56729.4876.
5. Kavand, A., Haeri, S.M., Raisianzadeh, J., et al., *Seismic behavior of a dolphin-type berth subjected to liquefaction induced lateral spreading: 1g large scale shake table testing and numerical simulations.* Soil Dynamics and Earthquake Engineering, 2021. **140**: p. 106450 DOI: https://doi.org/10.1016/j.soildyn.2020.106450.
6. Gao, J., Zhang, X., Liu, J., et al., *Numerical and experimental assessment of thermal performance of vertical energy piles: an application.* Applied Energy, 2008. **85**(10): p. 901-910 DOI: https://doi.org/10.1016/j.apenergy.2008.02.010.
7. Zarrella, A., De Carli, M., and Galgaro, A., *Thermal performance of two types of energy foundation pile: Helical pipe and triple U-tube.* Applied Thermal Engineering, 2013. **61**(2): p. 301-310 DOI: https://doi.org/10.1016/j.applthermaleng.2013.08.011.
8. Park, S., Lee, D., Choi, H.-J., et al., *Relative constructability and thermal performance of cast-in-place concrete energy pile: Coil-type GHEX (ground heat exchanger).* Energy, 2015. **81**: p. 56-66 DOI: https://doi.org/10.1016/j.energy.2014.08.012.
9. Yang, W., Lu, P., and Chen, Y., *Laboratory investigations of the thermal performance of an energy pile with spiral coil ground heat exchanger.* Energy and Buildings, 2016. **128**: p. 491-502 DOI: https://doi.org/10.1016/j.enbuild.2016.07.012.
10. Lee, S., Park, S., Kim, D., et al., *Dual performance of novel steel pipe heat exchangers equipped in cast-in-place energy pile.* Energy and Buildings, 2021. **234**: p. 110725 DOI: https://doi.org/10.1016/j.enbuild.2021.110725.
11. Moradshahi, A., Faizal, M., Bouazza, A., et al., *Effect of nearby piles and soil properties on thermal behaviour of a field-scale energy pile.* Canadian Geotechnical Journal, 2021. **58**(9): p. 1351-1364 DOI: https://doi.org/10.1139/cgj-2020-0353.
12. Bergström, A., Javed, S., and Dijkstra, J., *Field test of a floating thermal pile in sensitive clay.* Géotechnique, 2021. **71**(4): p. 334-345 DOI: https://doi.org/10.1680/jgeot.19.P.094.

13. Fang, J., Kong, G., Meng, Y., et al., *Thermomechanical behavior of energy piles and interactions within energy pile–raft foundations.* Journal of Geotechnical and Geoenvironmental Engineering, 2020. **146**(9): p. 04020079 DOI: https://doi.org/10.1061/(ASCE)GT.1943-5606.0002333.
14. Ren, L.-w., Xu, J., Kong, G.-q., et al., *Field tests on thermal response characteristics of micro-steel-pipe pile under multiple temperature cycles.* Renewable Energy, 2020. **147**: p. 1098-1106 DOI: https://doi.org/10.1016/j.renene.2019.09.084.
15. Jensen-Page, L., Loveridge, F., and Narsilio, G.A., *Thermal response testing of large diameter energy piles.* Energies, 2019. **12**(14): p. 2700 DOI: https://doi.org/10.3390/en12142700.
16. Senejani, H.H., Ghasemi-Fare, O., Cherati, D.Y., et al. *Investigation of thermo-mechanical response of a geothermal pile through a small-scale physical modelling*. in *E3S Web of Conferences*. 2020. EDP Sciences DOI: https://doi.org/10.1051/e3sconf/202020505016.
17. Ng, C.W.W., Farivar, A., Gomaa, S.M.M.H., et al., *Performance of elevated energy pile groups with different pile spacing in clay subjected to cyclic non-symmetrical thermal loading.* Renewable Energy, 2021a. **172**: p. 998-1012 DOI: https://doi.org/10.1016/j.renene.2021.03.108.
18. Ng, C.W., Farivar, A., Gomaa, S.M., et al., *Centrifuge modeling of cyclic nonsymmetrical thermally loaded energy pile groups in clay.* Journal of Geotechnical and Geoenvironmental Engineering, 2021b. **147**(12): p. 04021146 DOI: https://doi.org/10.1061/(ASCE)GT.1943-5606.0002689.
19. Ghaaowd, I. and McCartney, J.S., *Centrifuge modeling methodology for energy pile pullout from saturated soft clay.* Geotechnical Testing Journal, 2022. **45**(2): p. 20210062-20210062 DOI: https://doi.org/10.1520/gtj20210062.
20. Jafarzadeh, F. and Afzalsoltani, S. *Energy Piles, Applications and Research Aspects: An Investigation on the Behavior of a Single Energy Pile in Dry Condition*. in *International Conference on Geotechnical Engineering-IRAQ*. 2022. Springer DOI: https://doi.org/10.1007/978-981-19-7358-1_23.
21. Jafarzadeh, F. and Afzalsoltani, S., *Unsymmetrical thermal loading effects on a 2× 2 pile-group: 1g physical modeling approach*, in *Smart Geotechnics for Smart Societies*. 2023, CRC Press. p. 2197-2200 DOI: https://doi.org/10.1201/9781003299127.
22. Afzalsoltani, S. and Jafarzadeh, F., *The effect of mechanical surcharge on single energy pile foundations: 1g physical modeling*, in *7th International Young Geotechnical Engineers Conference*. 2022: Sydney, Australia.
23. Jafarzadeh, F., Afzalsoltani, S., Arbab, A., et al., *1g Physical Modeling of a Single Heat-Exchanger pile in Silty Sand* in *20 th International Conference on Soil Mechanics and Geotechnical Engineering*. 2022: Sydney, Australia.
24. Sutman, M., Brettmann, T., and Olgun, C.G., *Full-scale in-situ tests on energy piles: Head and base-restraining effects on the structural behaviour of three energy piles.* Geomechanics for Energy and the Environment, 2019. **18**: p. 56-68 DOI: https://doi.org/10.1016/j.gete.2018.08.002.
25. Ng, C.W.W., Shi, C., Gunawan, A., et al., *Centrifuge modelling of heating effects on energy pile performance in saturated sand.* Canadian Geotechnical Journal, 2015. **52**(8): p. 1045-1057 DOI: https://doi.org/10.1139/cgj-2014-0301.
26. Nguyen, V.T., Tang, A.M., and Pereira, J.-M., *Long-term thermo-mechanical behavior of energy pile in dry sand.* Acta Geotechnica, 2017. **12**(4): p. 729-737 DOI: https://doi.org/10.1007/s11440-017-0539-z.
27. Foglia, A., Abdel-Rahman, K., Wisotzki, E., et al., *Large-scale model tests of a single pile and two-pile groups for an offshore platform in sand.* Canadian Geotechnical Journal, 2021. **99**(999): p. 1825-1838 DOI: https://doi.org/10.1139/cgj-2020-0224.
28. Yang, W., Qiang, Y., Ju, L., et al., *Numerical evaluations on the effects of different factors on thermo-mechanical behaviour of an energy pile group.* Computers and Geotechnics, 2023. **162**: p. 105664 DOI: https://doi.org/10.1016/j.compgeo.2023.105664.
29. Iai, S., *Similitude for shaking table tests on soil-structure-fluid model in 1g gravitational field.* Soils and Foundations, 1989. **29**(1): p. 105-118 DOI: https://doi.org/10.3208/sandf1972.29.105.
30. Iai, S., Tobita, T., and Nakahara, T., *Generalised scaling relations for dynamic centrifuge tests.* Geotechnique, 2005. **55**(5): p. 355-362 DOI: https://doi.org/10.1680/geot.2005.55.5.355.

31. Oliver, M.A. and Webster, R., *Kriging: a method of interpolation for geographical information systems.* International Journal of Geographical Information System, 1990. **4**(3): p. 313-332 DOI: https://doi.org/10.1080/02693799008941549.
32. BSI, *BS EN 1997-1: 2004. Eurocode 7. Geotechnical design. General rules*. 2004, BSI London, UK DOI: https://doi.org/10.3403/03181153.
33. Boussinesq, J., *Application des potentiels à l'étude de l'équilibre et du mouvement des solides élastiques: principalement au calcul des déformations et des pressions que produisent, dans ces solides, des efforts quelconques exercés sur une petite partie de leur surface ou de leur intérieur: mémoire suivi de notes étendues sur divers points de physique, mathematique et d'analyse*. Vol. 4. 1885: Gauthier-Villars.
34. Sadek, M. and Shahrour, I., *Use of the Boussinesq solution in geotechnical and road engineering: influence of plasticity.* Comptes Rendus Mécanique, 2007. **335**(9-10): p. 516-520 DOI: https://doi.org/10.1016/j.crme.2007.08.007.

Prof. Fardin Jafarzadeh has established himself as a prominent figure in geotechnical engineering, with over 25 years of academic and industrial experience. He received his PhD. degree in Geotechnical Engineering from Tohoku University, Japan; in 1995. He is an Associate Professor in the Department of Civil Engineering at Sharif University of Technology (SUT), recognized as a leading institution in Asia. Dr. Jafarzadeh has been a member of the SUT faculty since 1996 and currently serves as the President of the Iranian Geotechnical Society (IGS), a position he has held since 2020. Dr. Jafarzadeh's research expertise spans various fields of geotechnical engineering, including soil dynamics and geotechnical earthquake engineering, ground improvement, unsaturated soil mechanics, physical modeling of energy piles, earth, and rockfill dams, constitutive modeling, and monitoring & retrofitting of geotechnical structures. He has been the Head of the Advanced Geotechnical Laboratory at SUT since 2014, actively overseeing the installation and upgrade of advanced laboratory equipment for element tests. In 2006, he established the Physical Modeling Laboratory to investigate the static and dynamic behavior of soil in geotechnical earthquake engineering and geothermal energy piles. Dr. Jafarzadeh's research findings have been published in over 100 articles in top-tier scholarly journals and peer-reviewed conference proceedings. He has also supervised more than 70 MS. and 10 Ph.D. students, mentoring the next generation of geotechnical engineers.

Sina Afzalsoltani is a PhD candidate at the Sharif University of Technology (SUT) in Tehran, Iran. He received a bachelor's degree in Civil Engineering from Amirkabir University (Tehran Polytechnic) and a master's degree in Geotechnical Engineering from SUT. He is interested in deep foundations, physical modeling, thermo-hydro-mechanical behavior of geomaterial and energy geotechnics. He has also been involved in several deep excavation projects in Tehran and currently collaborates with the headquarters office of the Construction Engineering Organization of Tehran province as a senior geotechnical engineer.

Table 1 Test plan

Test name	Number of energy piles	Soil type	Mechanical surcharge (kg)	Energy pile temperature (°C)
Group1	1	Air-dried silty sand (Dr=70%)	41.5	21.5±6 (10 cycles)
Group2	2	Air-dried silty sand (Dr=70%)	41.5	21.5±6 (10 cycles)
Group3	3	Air-dried silty sand (Dr=70%)	41.5	21.5±6 (10 cycles)

Table 2 Adopted scaling factors in the present study

Hydro-Mechanical quantities [29, 30]		**Thermal quantities**	
Quantity	**Scaling factors (prototype/model)**	**Quantity**	**Scaling factors (prototype/model)**
	$\lambda_\theta = \lambda_\rho = 1$		$\lambda_\theta = \lambda_\rho = 1$
	$\lambda_\varepsilon = \lambda^{0.5}$		$\lambda_\varepsilon = \lambda^{0.5}$

Acceleration	1	Temperature	λ_θ
Length	λ	Time (Diffusion)	λ^2
Density	$\lambda\rho$	Thermal expansion coefficient	$\lambda_\varepsilon / \lambda_\theta$
Time (Dynamic)	$(\lambda\lambda_\varepsilon)^{0.5}$	Thermal conductivity	1
Displacement	$\lambda\lambda_\varepsilon$	Thermal diffusivity	1
Stress	$\lambda\lambda_\rho$	Specific heat	1
Strain	λ_ε	Energy (heat)	$\lambda^3\lambda_\rho\lambda_\theta$
Stiffness	$\lambda\lambda_\rho / \lambda_\varepsilon$		
Force	$\lambda^3\lambda_\rho$		
Energy (mechanical)	$\lambda^4\lambda_\rho\lambda_\varepsilon$		

Table 3 Mechanical specifications of the piles in prototype and in the physical model

Assumed prototype pile (concrete pile with circular section)			
E(GPa)	Diameter(cm)	I(cm^4)	Section area-A (cm^2)
25	60	635850	2826
Mathematically required model pile specifications			
Quantity	Scaling factor	Prototype	Model
EI ($kN.m^2$)	$\lambda^{4.5} = 20^{4.5}$	158962.5	0.222156847
EA (kN)	$\lambda^{2.5} = 20^{2.5}$	7065000	3949.455065
Adopted model pile specifications			

Outer diameter (cm)	2
Wall thickness (cm)	0.12
Inner diameter (cm)	1.76
$I_{model}(cm^4)$	0.314239142
$A_{model}(cm^2)$	0.708384
$E_{Aluminum}$ (GPa)	70
EI_{model}	0.2199674
EA_{model}	4958.688

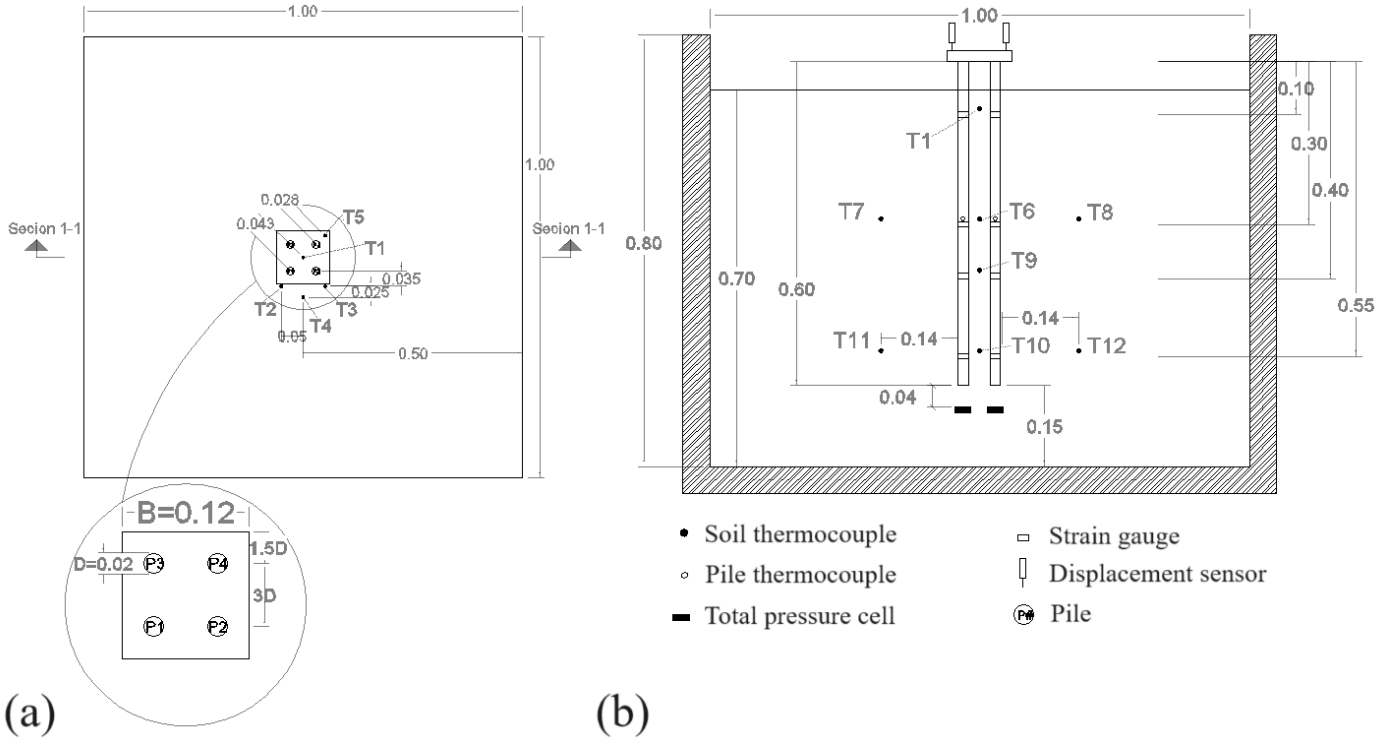

Fig. 1 Schematic views of the model configuration; a) plan view and b) section 1-1

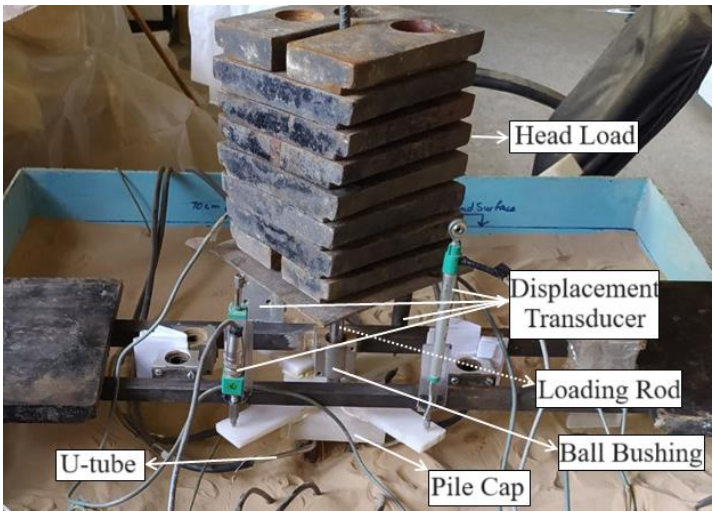

Fig. 2 Pile Cap and loading mechanism

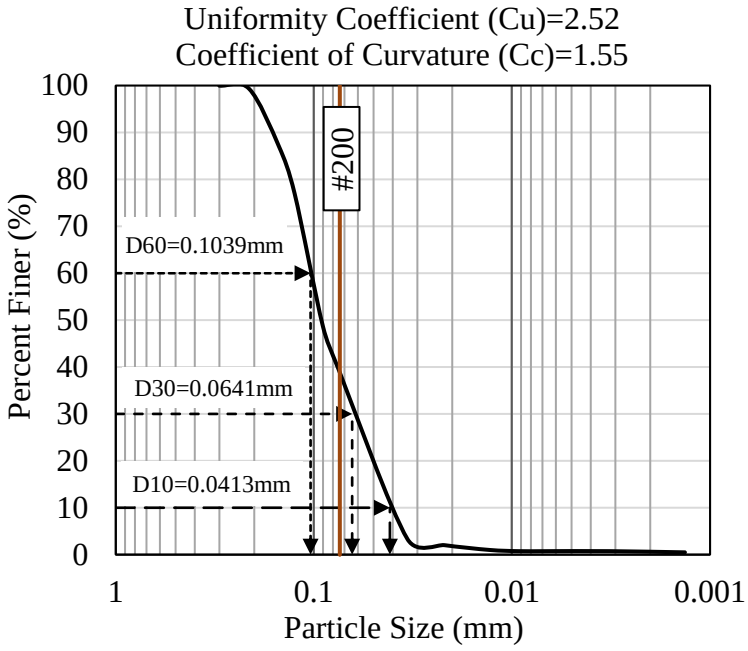

Fig. 3 Particle size distribution analysis of the model ground

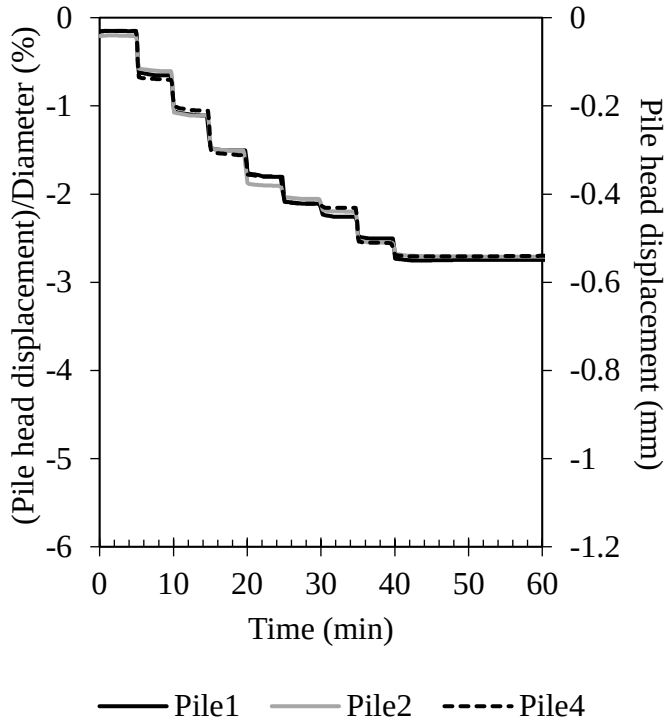

Fig. 4 Time history of pile head displacement for different piles of test "Group1" due to mechanical loading of the group before the onset of thermal loading

Fig. 5 profiles of axial force along piles plotted for different dead loads on the pile group during stepwise mechanical loading at room temperature: a) Pile1 in test “Group1”; b) Pile1 in test “Group2”and c) Pile1 in test “Group3”

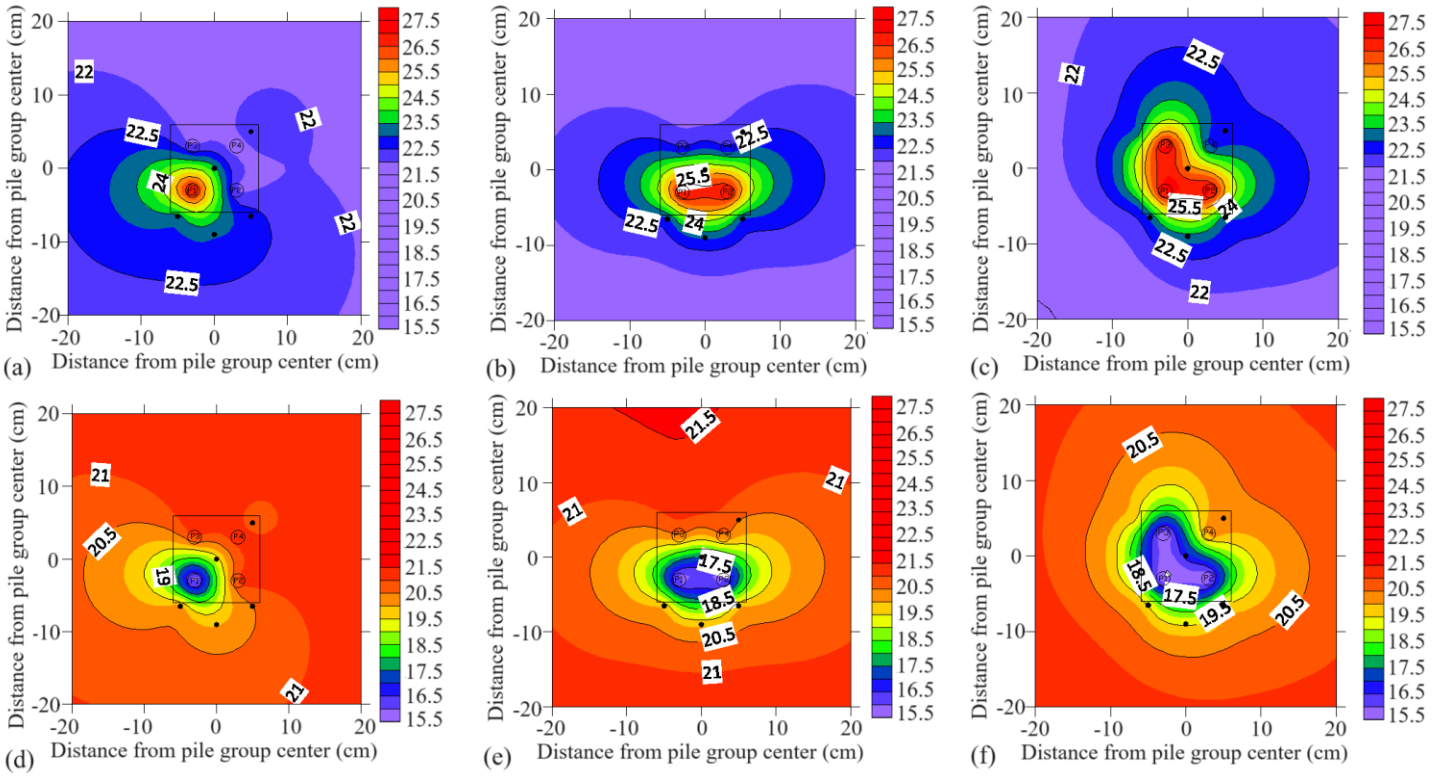

Fig. 6 Contours of soil temperature at depth of 5cm below surface at the end of first heating phase in tests a) Group1, b) Group2 and c) Group3 and at the end of first cooling phase in tests d) Group1, e) Group2 and f) Group3

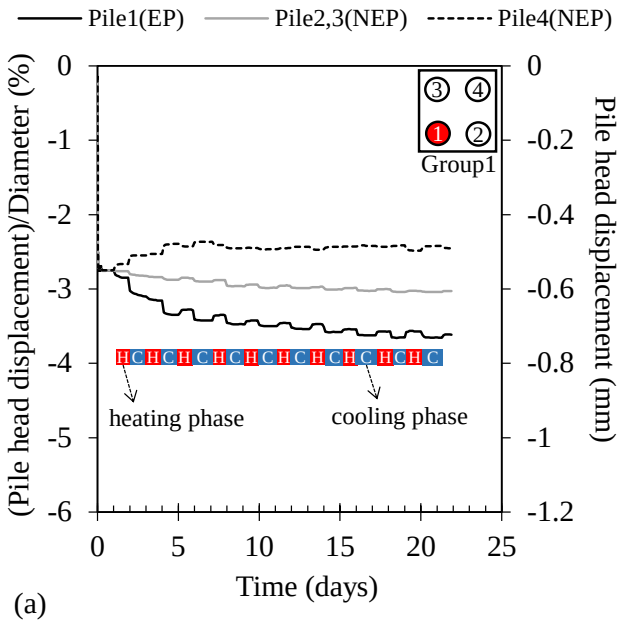
Pile1(EP)
Pile2,3(NEP)
Pile4(NEP)
(Pile head displacement)/Diameter (%)
Pile head displacement (mm)
Time (days)
Group1
heating phase
cooling phase

(a)

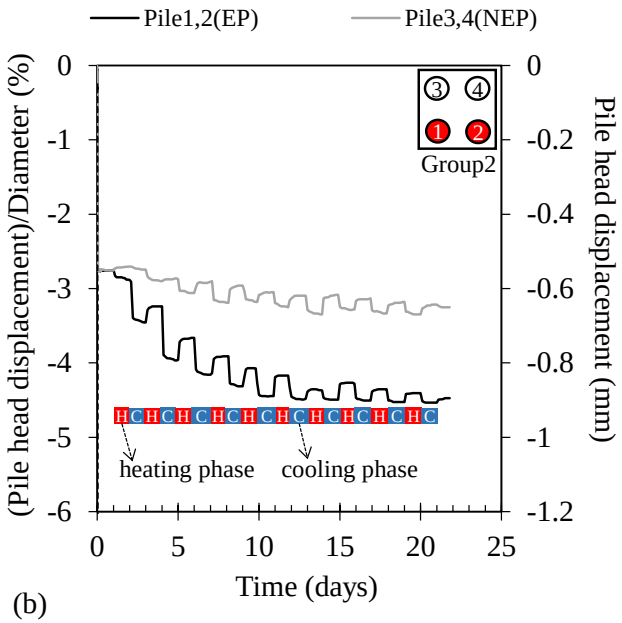
Pile1,2(EP)
Pile3,4(NEP)
(Pile head displacement)/Diameter (%)
Pile head displacement (mm)
Time (days)
Group2
heating phase
cooling phase

(b)

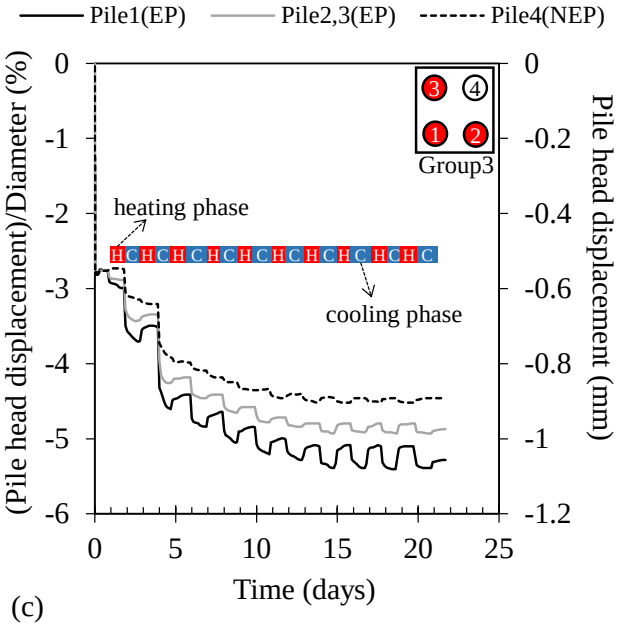
Pile1(EP)
Pile2,3(EP)
Pile4(NEP)
(Pile head displacement)/Diameter (%)
Pile head displacement (mm)
Time (days)
Group3
heating phase
cooling phase

(c)

Fig. 7 Time histories of pile head displacements for tests a) "Group1", b) "Group2" and c) "Group3"

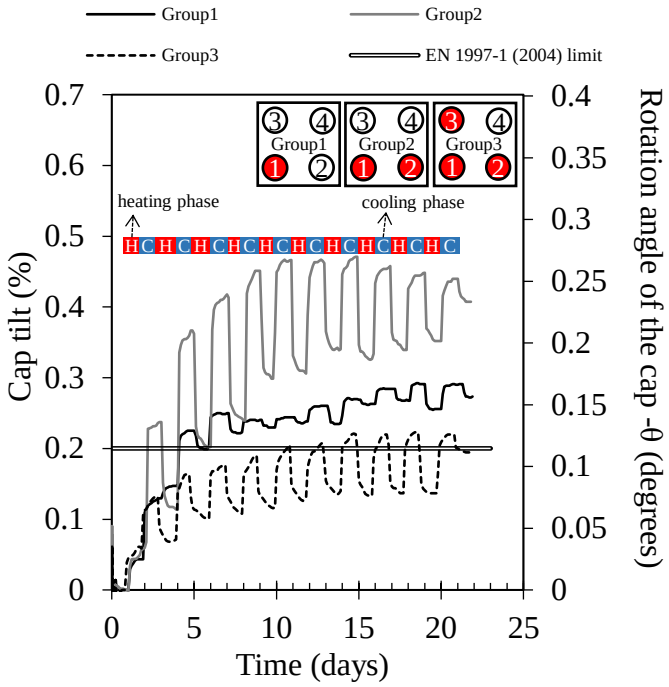

Fig. 8 Tilt and rotation angle of pile group caps in each test

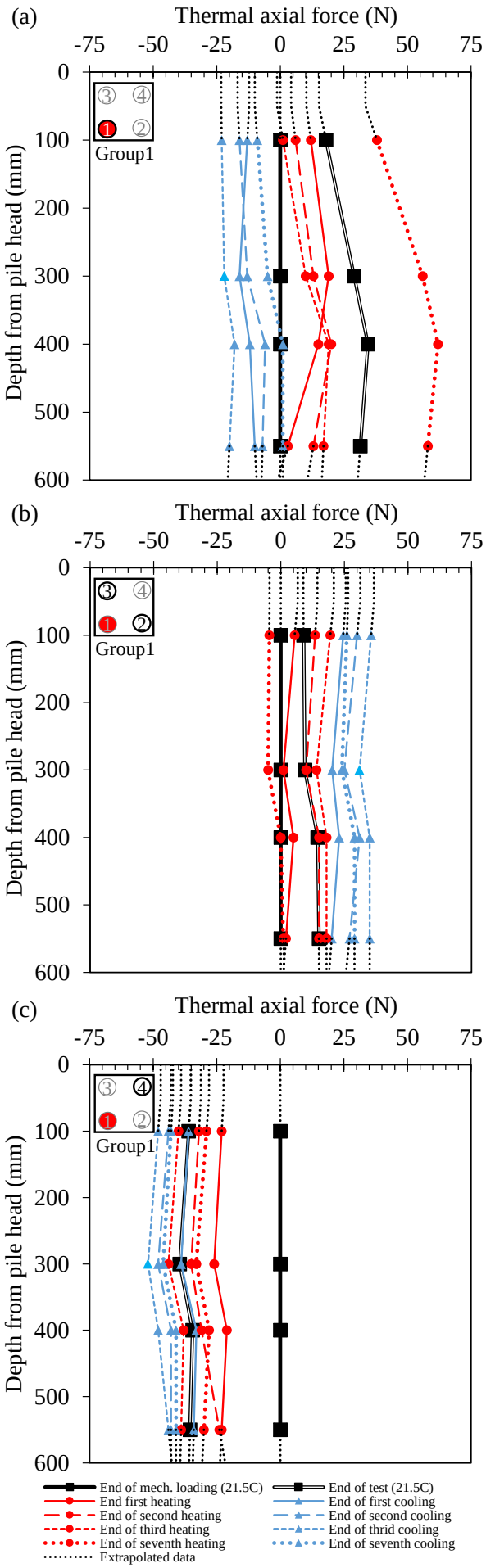
(a)
Thermal axial force (N)
-75 -50 -25 0 25 50 75
0 100 200 300 400 500 600
Depth from pile head (mm)
③ ④
① ②
Group1
(b)
Thermal axial force (N)
-75 -50 -25 0 25 50 75
0 100 200 300 400 500 600
Depth from pile head (mm)
③ ④
① ②
Group1
(c)
Thermal axial force (N)
-75 -50 -25 0 25 50 75
0 100 200 300 400 500 600
Depth from pile head (mm)
③ ④
① ②
Group1
End of mech. loading (21.5C)
End first heating
End of second heating
End of third heating
End of seventh heating
Extrapolated data
End of test (21.5C)
End of first cooling
End of second cooling
End of thrid cooling
End of seventh cooling

471

Fig. 9 Temperature-induced axial force profiles along a) Pile1, b) Pile2,3 and c) Pile4 for test "Group1"

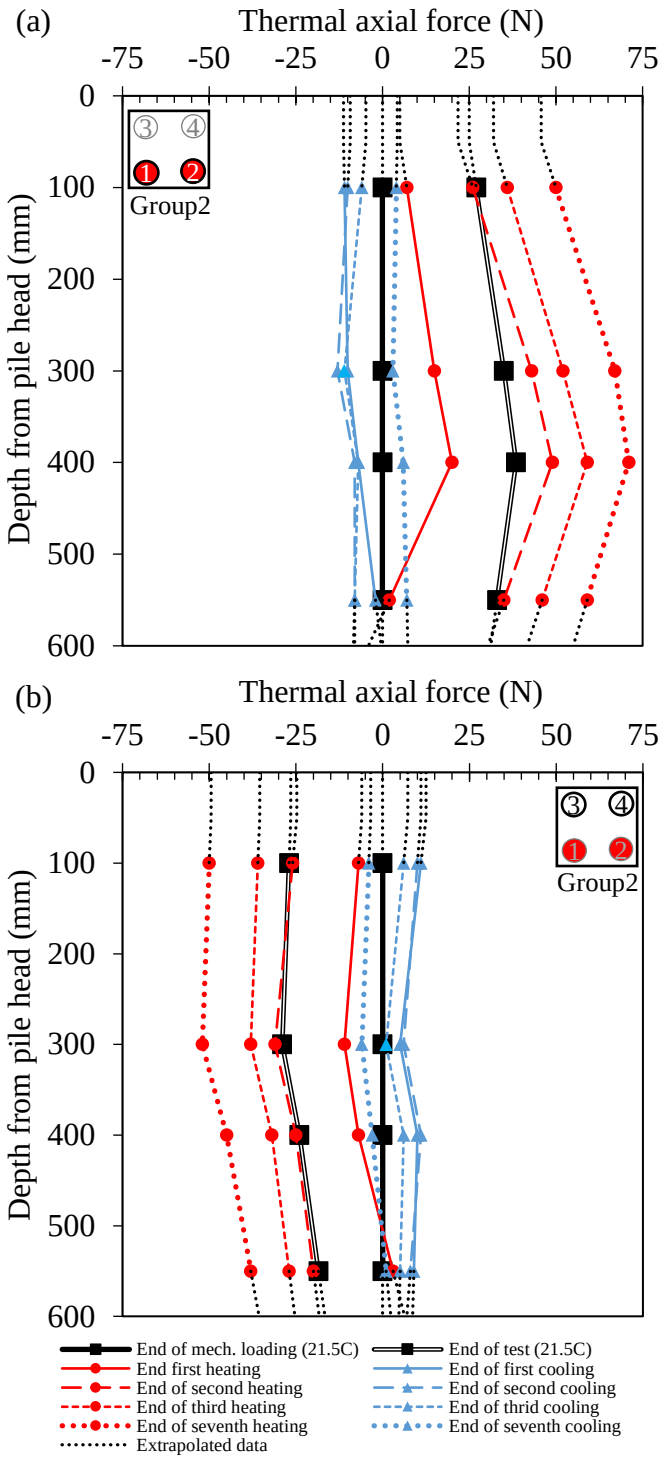

Fig. 10 Temperature-induced axial force profiles along a) Pile1,2 and b) Pile3,4 for test "Group2"

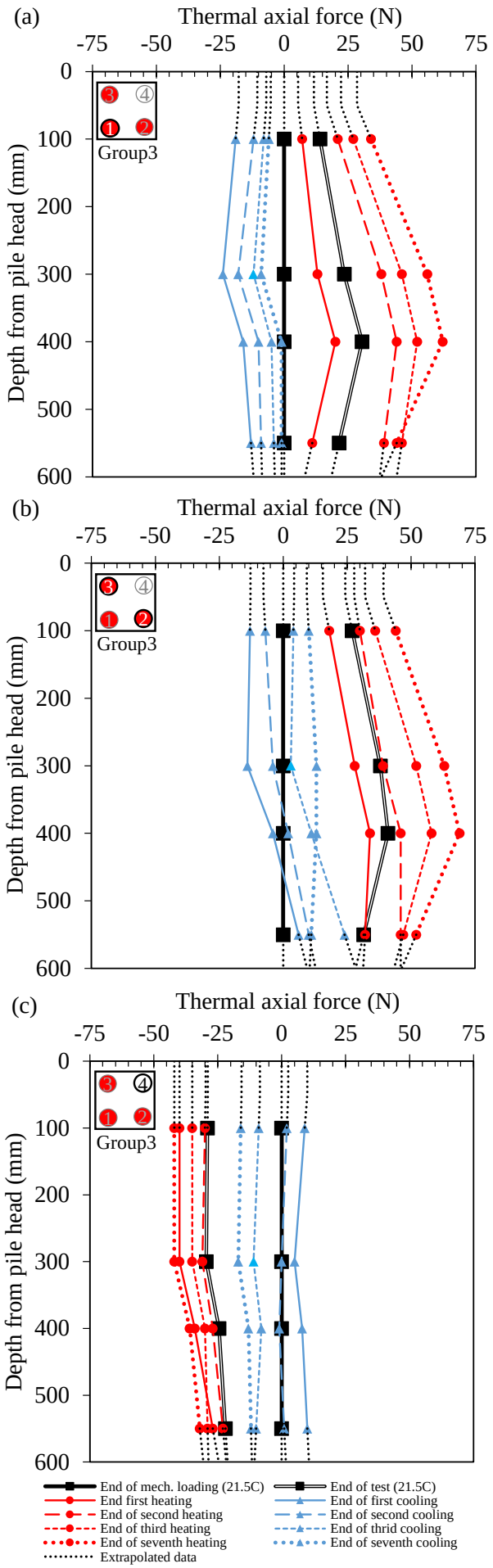
(a)
Thermal axial force (N)
-75 -50 -25 0 25 50 75
0 100 200 300 400 500 600
Depth from pile head (mm)
3 4
1 2
Group3
(b)
Thermal axial force (N)
-75 -50 -25 0 25 50 75
0 100 200 300 400 500 600
Depth from pile head (mm)
3 4
1 2
Group3
(c)
Thermal axial force (N)
-75 -50 -25 0 25 50 75
0 100 200 300 400 500 600
Depth from pile head (mm)
3 4
1 2
Group3
End of mech. loading (21.5C)
End first heating
End of second heating
End of third heating
End of seventh heating
Extrapolated data
End of test (21.5C)
End of first cooling
End of second cooling
End of thrid cooling
End of seventh cooling

Fig. 11 Temperature-induced axial force profiles along a) Pile1, b) Pile2,3 and c) Pile4 for test "Group3"

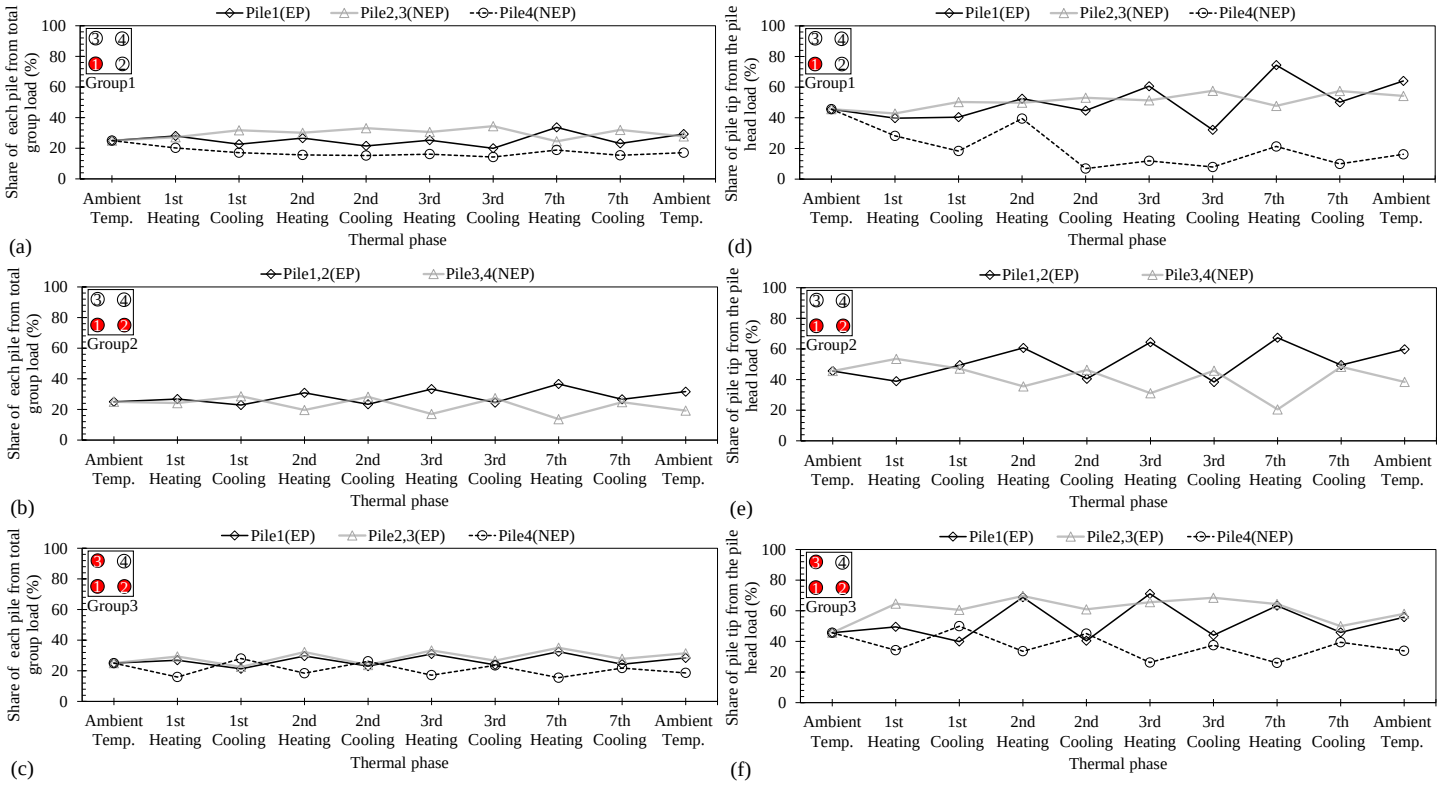

Fig. 12 Share of each pile from total mechanical head load on the group (415 N) for a) Group1, b) Group2, c) Group3 and share of pile tip from each pile's head load for d) Group1, e) Group2 and f) Group3

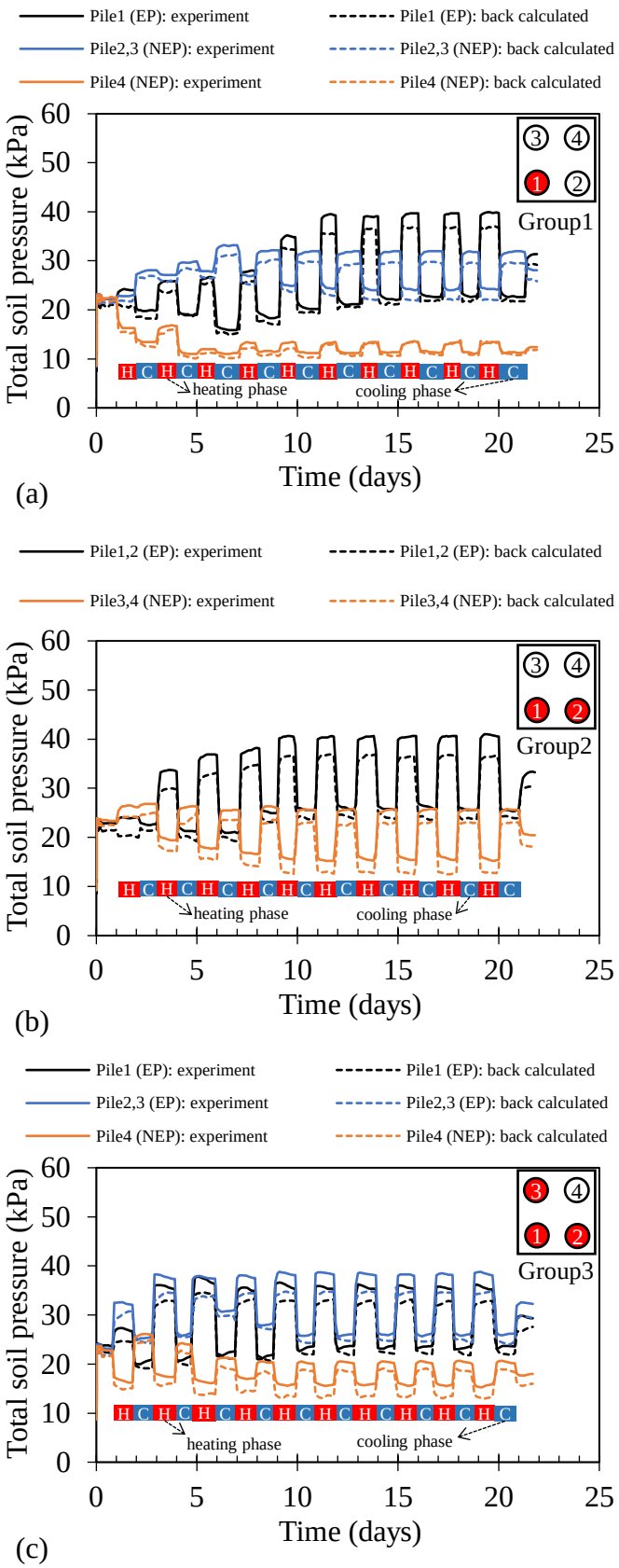

Fig. 13 Time histories of total soil pressure under different piles in each test

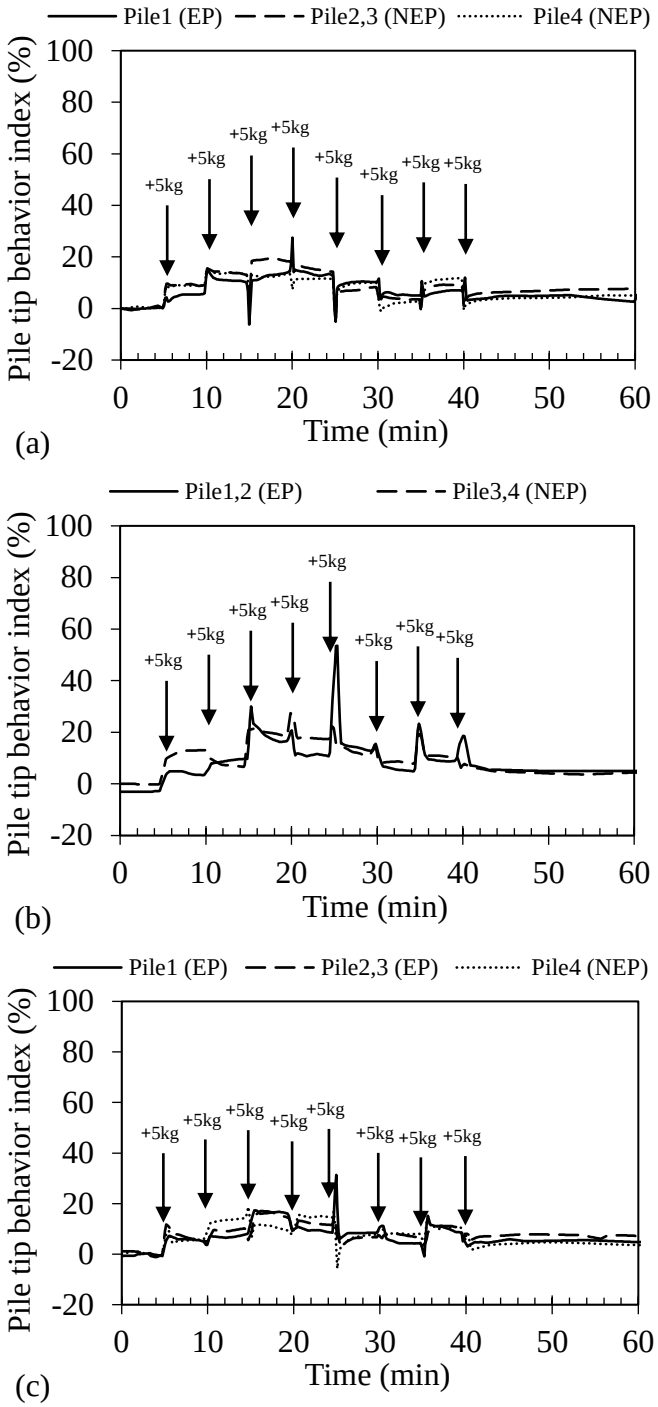

Fig. 14 Time history of pile tip behavior index before the onset of thermal cycling and during mechanical loading of the pile group for different piles in tests: a) ”Group1”, b) “Group2” and c) “Group3”

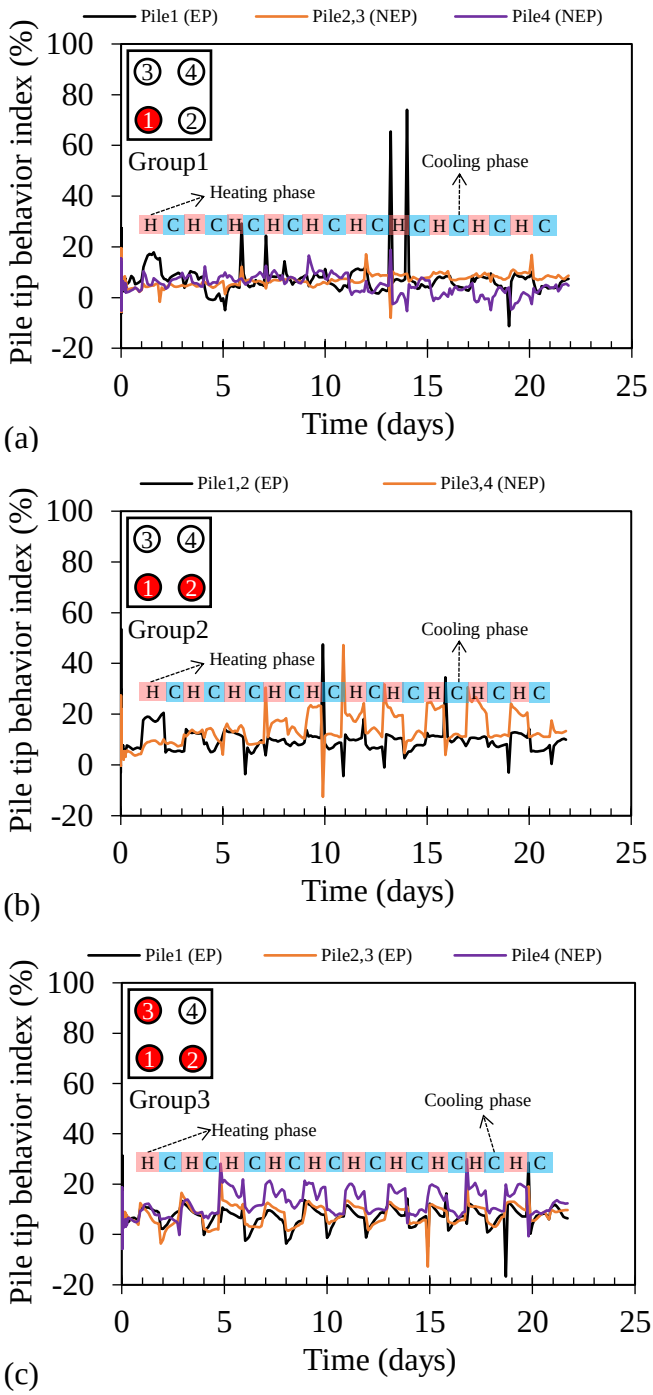

Fig. 15 Time history of the pile tip behavior index for different piles of each test